



Contents lists available at ScienceDirect

Journal of Biomechanics

journal homepage: [www.elsevier.com/locate/jbiomech](http://www.elsevier.com/locate/jbiomech)  
[www.JBiomech.com](http://www.JBiomech.com)

## Spatial resolution of spontaneous accelerations in reaching tasks

Michael Wininger<sup>a,\*</sup>, Nam-Hun Kim<sup>a,b</sup>, William Craelius<sup>a</sup>

<sup>a</sup> Department of Biomedical Engineering, Rutgers, The State University of New Jersey, Piscataway, NJ 08854, USA

<sup>b</sup> Department of Physical Medicine and Rehabilitation, University of Medicine and Dentistry of New Jersey, NJ, USA

### ARTICLE INFO

#### Article history:

Accepted 8 October 2008

#### Keywords:

Reaching  
Jerk  
Trajectory  
Arm  
Rehabilitation

### ABSTRACT

Reaching tasks are considered well-executed if they appear “smooth,” a quality that is typically quantified by its opposite, jerk, the rate of change of acceleration. While jerk is a theoretically sound measure, its application to spastic individuals sometimes yields counter-intuitive results, and does not reveal motor impairment across the workspace. To more generally quantify spontaneous accelerative transients (SATs) within a movement, a pseudo-wavelet transform was devised that iteratively compared angular trajectories to a series of straight-line approximants. Cumulative linear fit errors were expressed in terms of flexion angle, yielding an SAT map of the entire motion. To compare SAT maps with traditional smoothness measures, two scalar indices were extracted from them: residual excursion deviation (*RED*), representing the integral over  $\Delta\theta$  and the ratio of peak error to mean error (*PEME*) on the map. Fifteen subjects, including five subjects with chronic stroke performed elbow flexions throughout their entire ranges of motion,  $\Delta\theta$ , at a comfortable pace with their arms supported in the transverse plane. Maps revealed that stroke subjects were significantly less coordinated than controls, as measured both by *RED*:  $8.0 \pm 2.9 \times 10^{-3}$  versus  $3.1 \pm 0.8 \times 10^{-3}$  and *PEME*:  $6.6 \pm 0.9$  versus  $12.1 \pm 1.9$ , both  $P < 0.001$ . Comparable jerk metrics, including integrated average jerk, did not report a significant performance deficit at the  $P < 0.05$  level. Map metrics for all subjects were independent of average velocity (correlation with  $\dot{\theta}$ :  $\rho \leq 0.31$ ), but jerk-based metrics for stroke subjects were spuriously covariant with velocity  $\rho = 0.85$ , which may relate to the significantly higher mean arrest period ratio in stroke subjects ( $0.26 \pm 0.19$  versus  $0.09 \pm 0.08$ ,  $P < 0.001$ ). We conclude that SAT maps provide reliable information on regional movement impairments at a wide range of proficiency levels.

© 2008 Elsevier Ltd. All rights reserved.

### 1. Introduction

Human motor proficiency is generally characterized in terms of smoothness in the movement record, which is a primary index of neural recovery following stroke (Trombly, 1993; Platz et al., 1994; Kahn et al., 2001; Rohrer et al., 2002). Traditional time-domain metrics of smoothness such as jerk are convenient for comparative purposes, but scalar quantities based on temporal information are susceptible to artefact associated with signal processing techniques (Hsiang et al., 1999; Dabroom and Khalil, 1999) and are opaque to the locality of performance deficits in space. Furthermore, jerk-based assessments occasionally report insignificant performance deficits in impaired cohorts, or even increased jerk with rehabilitation, contradicting other smoothness measures (Goldvasser et al., 2001; Rohrer et al., 2002).

Myriad neuromuscular effectors exhibit a positional dependence during normal reaching (Lan and Crago, 1994; Gottlieb et al., 2004; Pigeon et al., 1996; Kashima et al., 2000; Suzuki et al.,

2001), as well as reaching by hemiparetic subjects (Levin and Dimov, 1997; Levin et al., 2000; Ju et al., 2002; Hu et al., 2006). Whether, and to what degree this positional variability manifests biomechanically, is not well understood. In other words, how does task smoothness vary with position? To answer this question, a spatially sensitive smoothness measure is needed.

We present a method for producing maps of spontaneous accelerative transients (SATs) that depict motor performance throughout the entire range of motion (ROM) of a single joint, i.e. as a function of joint angle, not time. The method employs a pseudo-wavelet paradigm to detect regions of stable velocity and depicts SATs as bright bands against a black background. Assessment of the algorithm was performed on repetitive elbow flexions of chronic stroke patients as well as age- and gender-matched control subjects with no known neurological impairments. Scalar smoothness measures were derived quantifying morphological parameters of their SAT maps, allowing for comparisons to standard jerk metrics. This transformation into the angular domain eliminates residual error associated with the repeated differentiation of discrete-time data, and obviates systematic bias of time-domain smoothness metrics, such as jerk, due to prolonged *stall* behaviors (time spent at low angular

\* Corresponding author. Tel.: 732.445.1178; fax: +1 732.445.2369.  
E-mail address: [wininger@eden.rutgers.edu](mailto:wininger@eden.rutgers.edu) (M. Wininger).

velocities) typical of spastic movements. The present discussion is limited to single-joint elbow flexions, but can be extended to any single- or multi-joint movement.

2. Methods

2.1. Subjects and protocol

Fifteen volunteers were recruited to participate in this pilot study. Ten healthy subjects with no known neurological impairments, and five chronic stroke patients made a single visit (Table 1). Two subjects were left-dominant prior to stroke; all subjects were right-affected. Stroke subjects were selected on the basis of moderate impairment as measured by the Chedoke-McMaster Stroke Assessment score of between 3 and 4 on a 0–7 scale (7 = unimpaired), without regard to dominance. All subjects gave informed consent on based on the procedures approved by the IRB of Rutgers University.

Subjects were seated in the mechanical arm support and tracker (MAST), which supports the arm against gravity while recording angle of elbow flexion. Each control subject was seated with his/her dominant (right) arm in the MAST; each stroke subject used his/her affected arm. The elbow rested on a cushioned pad, and shoulder and wrist involvement was minimized by physical constraint. Instantaneous feedback of angular position was provided by an electronic dial-face display, though subjects were not explicitly instructed to attend to this display. After a familiarization session and adequate warm-up exercises, subjects were asked to perform cyclic flexion-extension repetitions at his/her own pace, maximizing smoothness within their maximal ROM,  $\Delta\theta$ .

2.2. Signal processing

The MAST-mounted goniometer recorded elbow motion with a resolution of  $\pm 0.05^\circ$  and was routed through a DAQ board (National Instruments, Austin TX) to a LabView (National Instruments) GUI. Raw data were processed bi-directionally with a 2nd-order lowpass Butterworth's filter with a 4 Hz cutoff prior to analysis. Individual flexions were extracted by automated detection of local minima in the trajectory trace, and edge effects were removed.

2.3. Linear segmentation

For any angular trajectory,  $\theta(t)$ , regional adherence to an iso-accelerative movement can be assessed by modeling excursion as a piecewise function,  $P$ , of  $j$

Table 1 Subject demography.

	Healthy N = 10	Stroke N = 5
Age	54.9 ± 14.2	47.7 ± 20.8
Gender	4M/6F	2M/3F
Months post-stroke		16 ± 8
Chedoke-McMaster arm score		3.4 ± 0.5

All healthy subjects were right-dominant, all stroke patients were right-affected (3 were right-dominant).

linear segments (Fig. 1). As  $j$  increases, departures from a smooth movement, in the form of SATs, will be detected as error to this linear fit. Each segment,  $k$ , transcribes a line with constant angular velocity linking all angles between  $\theta_k$  and  $\theta_{k+1}$  where  $k \in \mathbb{N} < j+1$  and  $\theta = \theta(\tau)$  such that  $\tau = T \cdot \{k-1/j\}$ ,  $T$  the total time of movement. Thus, the  $k$ th segment is given by

$$P_k = \left[ \frac{\theta_{k+1} - \theta_k}{(T/j)} \cdot \left( i - \frac{k-1}{j} T \right) \right] + \theta_k \tag{1}$$

where  $k = |G|:G \subset \{k-1/j\} < i/T$ .

2.4. Regional deviations from straight trajectory

Each linear segment was compared against the corresponding portion of the observed motion, and a regional error was calculated according to the Pearson product-moment correlation coefficient relating the observed motion to that of a straight-slope excursion

$$E_k = 1 - \rho(P_k, \theta_k) \tag{2}$$

where the correlation coefficient is given by

$$\rho = \frac{\langle P_k, \theta_k \rangle - (T/j) \bar{P}_k \bar{\theta}_k}{\left( (T/j) - 1 \right) \sigma_{P_k} \sigma_{\theta_k}} \tag{3}$$

where  $\langle P_k, \theta_k \rangle$  is the inner-product of the trajectory segment and its linear approximant. The correlation coefficient ranges from 0 (no correlation) to 1 (identical signals), thus  $E_k$  acts as a negative index of correlation. For segments containing SATs, departure from a linear trajectory approximant will be considerable, increasing the error. For each iteration,  $j$ , regional errors are written onto the appropriate loci of template vector  $V_j$ , spanning the ROM

$$V_{j\gamma} = E_k v \frac{k-1}{j} < \frac{\gamma}{v} \leq \frac{k}{j} \tag{4}$$

where  $\gamma$  is an assignment index within the  $j$ th row of  $V$  on to which the error is assigned along the degrees-dimension, yielding the transform into the angular domain. The resolution of  $V$  is determined by  $v$ , here 512 data points, yielding  $\sim 0.25^\circ$  window-size in a ROM of  $\Delta\theta = 120^\circ$  (Fig. 2). We define the spatial acceleration vector  $S$  as the sum across all iterations  $j = 1, \dots, N$ :

$$S_j = \sum_j^N V_{j\gamma} \tag{5}$$

where  $N$  is a limit arbitrarily chosen to be the iteration at which at least one segment comprises fewer than a pre-defined threshold minimum number of data points (here chosen to be equal to 3: below this, all straight-line models reflect the trivial straight-line connecting two adjacent samples) (Fig. 3). For all analyses,  $S$  is adjusted by subtracting the spatial acceleration minimum  $S_{\min}$

2.5. Comparison of scalar smoothness measures

The squared-magnitude of the time-change of acceleration was integrated over  $T$ :

$$|AJ| = \frac{1}{T} \int_T \left| \frac{d^3}{dt^3} \theta(t) \right|^2 dt, \tag{6}$$

yielding integrated average jerk ( $|AJ|$ ), a single scalar value of dys-coordination. The jerk integral is temporally normalized so as to mitigate the effects of movement

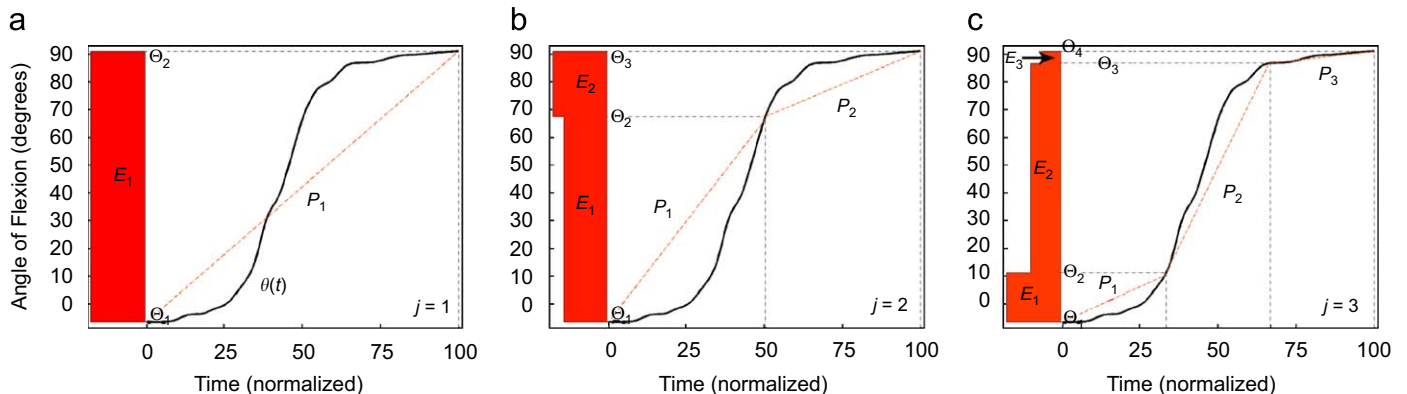
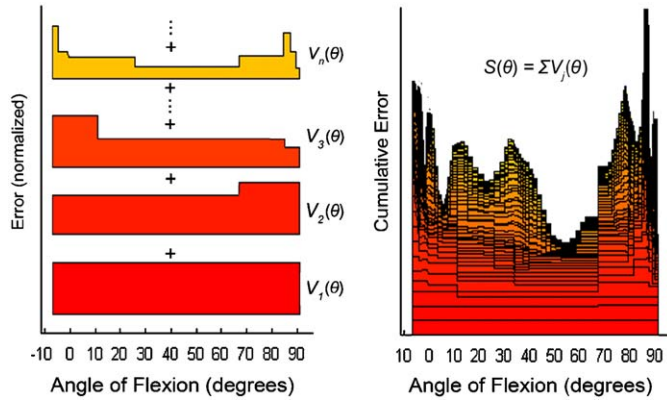
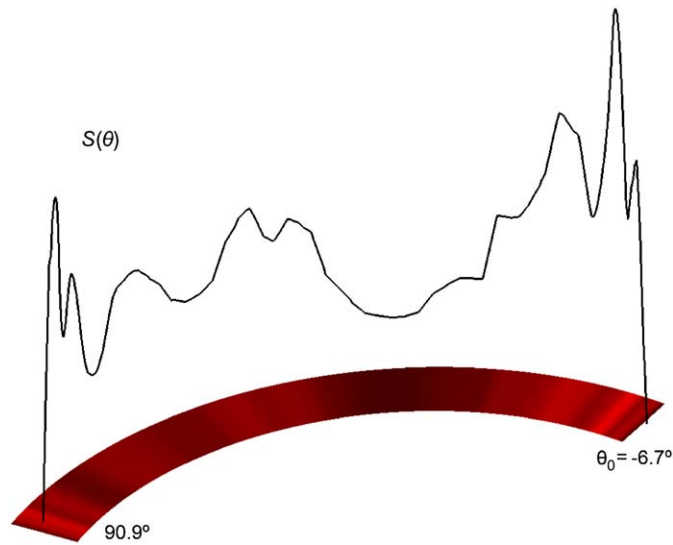


Fig. 1. Generation of the first three piece-wise comparisons  $P$  against a single flexion from a stroke subject. Comparison of recorded motion  $\theta(t)$  against a straight-line plot  $P_k$  (Eq. (1)), spanning  $T/j$  timepoints, representing zero acceleration. The dotted lines show even time partitions of time (into 1 section, halves, thirds, and so on), and the vertical bar plots  $V_j$  along the ordinate reflect regional error  $E_k$  of  $\theta$  to  $P_k$  (Eq. (2)).



**Fig. 2.** Summing  $V$  over  $j$  iterations results in a cumulative error plot, yielding spontaneous accelerative transient (SAT) map  $S(\theta)$  as the trace of peaks.



**Fig. 3.** Depiction of spatial error across the workspace. Cumulative error trace is plotted as a color-coded vector along the  $x$ - $y$  coordinates of the hand in space. Shown: sample error plot of elbow flexion in transverse plane. Colors range from black (least error) to red (greatest error) according to the peaks of  $S(\theta)$ . Figure reflects the time-domain data (angle of flexion vs. time) transformed into the angular-domain (cumulative error to straight-line approximants vs. angle of flexion).

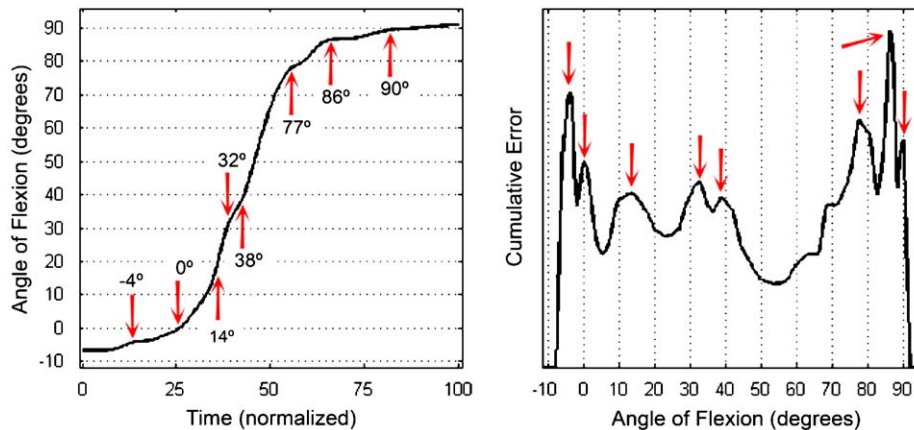


**Fig. 4.** Flexion motion performed by a stroke patient (CM level 3). Spontaneous accelerative transients (SATs) in the excursion trace are highlighted, as are their corresponding peaks in the cumulative error-to-straight-line plot.

speed on jerk score (Cozens and Bhakta, 2003). In concordance with standard practice, each differentiation was smoothed with filter characteristics identical to those defined above; trapezoidal integrals were computed.

For comparison purposes, the equivalent integration was performed on the spatial acceleration vector  $S$  over the angular range  $\Delta\theta$ . The regional excursion deviation (RED) represents the scalar magnitude of the spontaneous accelerations across the workspace and was defined as,

$$RED = \frac{1}{N} \int_{\Delta\theta} S(\theta) d\theta. \quad (7)$$

By normalizing to the number of segments,  $N$ ,  $RED$  is insensitive to different average velocities, and more generally allows for comparison across experiments by eliminating differences between sampling frequencies, and is analogous to temporal normalization of average jerk (Eq. (6)).

In order to determine the relative power of instances of least smoothness, the peak error-to-mean error ( $PEME$ ) ratio of maximum trace value (peak error to an iterated approximation as a straight-line segment in  $S$ , and maximum jerk in  $IAJ$ ) to trace means. Under the hypothesis that persons with impaired motor control would be prone to SATs throughout their range of motion, there should be several peaks within the  $S(\theta)$  and  $|d^3/dt^3\theta(t)|^2$  traces, in addition to the large peaks expected from movement onset and cessation. Integrated metrics  $RED$  and  $IAJ$  should thus increase due to the additional area under each curve, and the relative severity peaks associated with movement reversal should be muted by the increase in trace peak content, thus decreasing  $PEME$ .

Additionally, the number of peaks,  $\pi$ , were calculated. Group-wise differences were determined by the Wilcoxon rank-sum test.  $PEME_{S,J}$  and  $\pi_{S,J}$  will be subscripted to denote values computed in the angular ( $S(\theta)$ ) or time ( $J(t)$ ) domain. Integrated metrics ( $LAJ$  and  $RED$ ) as well as  $PEME$  and  $\pi$  are unit-less quantities reflecting area under a curve, a ratio and a tally, respectively. The mean arrest period ratio (MAPR), i.e. time spent at less than 10% maximum angular velocity to total movement duration, was calculated as  $(\dot{\theta}(t) < (\dot{\theta}_{max}/10))/T$ , (Beppu et al., 1984; Rohrer et al., 2002).

### 3. Results

A typical flexion trace from a stroke subject is shown in Fig. 4, with major inflections noted by arrows (Figs. 1–4 were generated from the same sample flexion). Note the correspondence of the inflections with peaks in spontaneous acceleration trace  $S(\theta)$  (arrows).

Comparing SAT maps of controls and stroke subjects, it can be seen from Fig. 5 that controls tended to produce doubly peaked profiles, with thin bands only at the onset and cessation of activity (i.e. at plot extrema). In contrast, stroke subjects produced large transient accelerations at intermediary angles.

As expected, stroke subjects performed single-joint reaching tasks with compromised range of motion ( $80 \pm 3^\circ$ , versus  $91 \pm 4^\circ$  for healthy subjects,  $P < 0.001$ , Table 2), and produced movements comprising greater periods of stall activity, as indicated by the MAPR of  $0.26 \pm 0.19$  versus  $0.09 \pm 0.08$ ;  $P < 0.001$ , (Table 3).

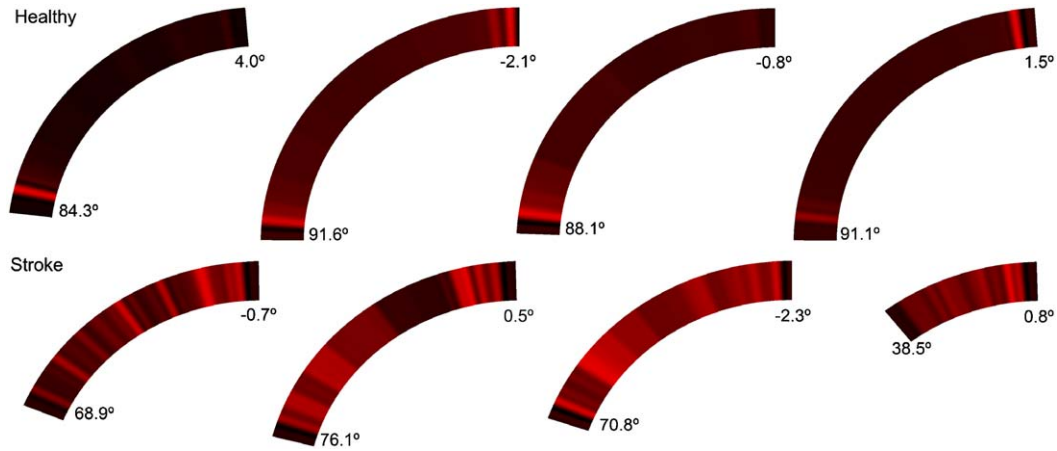


**Fig. 5.** Sample traces from four unimpaired subjects (*Top*) and four chronic stroke patients (*Bottom*). The bright bands at the plot extrema reflect motion initiation and cessation. For stroke subjects, intermediary activity produces SATs of equal or greater magnitude to that of motion onset and cessation.

**Table 2**  
Motor performance parameters and  $S(\theta)$ -derived metrics.

	Range of motion ( $\Delta\theta$ )	Curve area		Curve ratio (max:mean)		Curve peak count	
		RED ( $\times 10^{-3}$ )	IAJ ( $\times 10^{-5}$ )	PEME <sub>s</sub>	PEME <sub>j</sub> ( $\times 10^{-5}$ )	$\pi_s$	$\pi_j$
Healthy	91.0 ± 3.8	3.1 ± 0.8	9.0 ± 6.7	12.1 ± 1.9	9.9 ± 7.7	9.3 ± 0.9	14.4 ± 4.5
Stroke	80.0 ± 3.0	8.0 ± 2.9	40.6 ± 46.9	6.6 ± 0.9	42.8 ± 49.4	9.9 ± 1.6	9.9 ± 5.7
Signif.	$P \approx 0.028$	$P \approx 6.7 \times 10^{-4}$	$P \approx 0.25$	$P \approx 6.6 \times 10^{-4}$	$P \approx 0.77$	$P \approx 0.79$	$P \approx 0.10$

**Table 3**  
Correlation to average velocity: motor performance parameters and  $S(\theta)$ -derived metrics.

	MAPR(10%)	Curve area		Curve ratio (max:mean)	
		RED	IAJ	PEME <sub>s</sub>	PEME <sub>j</sub>
Healthy	0.09 ± 0.08	-0.22	0.40	0.03	0.38
Stroke	0.26 ± 0.19*	0.07	0.85	0.31	0.85

\*  $P < 0.001$ .

Both scalars derived from SAT maps, RED and PEME<sub>s</sub>, revealed significant dyscoordination in the stroke group, at the  $P < 0.001$  level, in contrast to those derived from jerk, IAJ and PEME<sub>j</sub>, which did not reach significance at the  $P < 0.05$  level, as shown in Table 2. Trace peak counts, however, yielded similar results using both methods, with  $\pi_s = 9.9 \pm 1.6$  versus  $9.3 \pm 0.9$ , and  $\pi_j = 9.9 \pm 5.7$  versus  $14.4 \pm 4.5$  for stroke and control subjects, respectively.

#### 4. Discussion

The finding of significantly reduced smoothness within a small cohort of hemiparetic subjects demonstrates the discriminative power of scalar metrics derived from SAT maps as opposed to jerk-based metrics, which failed to discriminate between cohorts at the  $P < 0.05$  level, and do not reliably co-vary with other smoothness measures (Goldvasser et al., 2001; Rohrer et al., 2002; Cozens and Bhakta, 2003).

We propose that the inability of jerk to resolve a significant performance deficit in a cohort with large MAPR is due to curve normalization by time (Eq. (6)). An antithetical relationship between MAPR and normalized average jerk has been reported elsewhere, but causality has been attributed to various other

phenomena, such as the blending of sub-movements (Krebs et al., 1999; Goldvasser et al., 2001; Rohrer et al., 2002). Jerk normalization is considered necessary in order to eliminate bias due to average velocity or total range of motion (Rohrer et al., 2002; Cozens and Bhakta, 2003), and alternate formulations have been proposed where total movement duration is penalized (Hoff, 1994; Engelbrecht, 2001). However, in movements with prolific stall behavior, time-normalized jerk and related metrics may actually decrease in spastic movements due to a preponderance of zero-jerk activity during stall periods.

This phenomenon is simulated in a sample flexion trace recorded from a healthy individual (Fig. 6). Integrating over time to  $T_1 = 2.5$ s, the area under the jerk trace of the flexion (*Top Left*) will yield jerk score  $J_1 = 83$ . Artificially introducing two stall periods of duration  $T = 0.25 T_1$  into the positional trace (inset, *Top Right*), punctuates the jerk trace by 0-jerk segments associated with the period of no movement. The area under the curve remains the same however, because the integration is over a longer duration  $T_2 = T_2 + 2 T = 3.75$ s; thus the jerk score equates  $J_2 = J_1$ . Temporally normalizing the jerk waveforms places the long trace into the same temporal bounds as the short trace, decreasing the area under the curve as the peaks of the long trace are “squeezed” to  $\frac{2}{3}$  their original width in order to accommodate the  $\frac{1}{3} T^*$  of stall activity (*Bottom*).

Comparing smoothness measures with regard to their dependence on movement speed, it was found that for healthy subjects jerk-based metrics correlated poorly to average velocity, as expected:  $\rho(\text{IAJ}, \dot{\theta}) = 0.4$ ,  $\rho(\text{PEME}_j, \dot{\theta}) = 0.38$  (Table 3). For stroke subjects, however, the jerk metrics were strongly correlated with average velocity:  $\rho(\text{IAJ}, \dot{\theta}) = \rho(\text{PEME}_j, \dot{\theta}) = 0.85$ , likely due to the MAPR value for stroke subjects being 3 times greater than that for controls. Thus, as stall periods decrease average velocity, IAJ is concomitantly reduced, forcing covariation between IAJ and  $\dot{\theta}$ . Compounding the problem is the high variability of MAPR that passes on to intra-subject jerk variability.

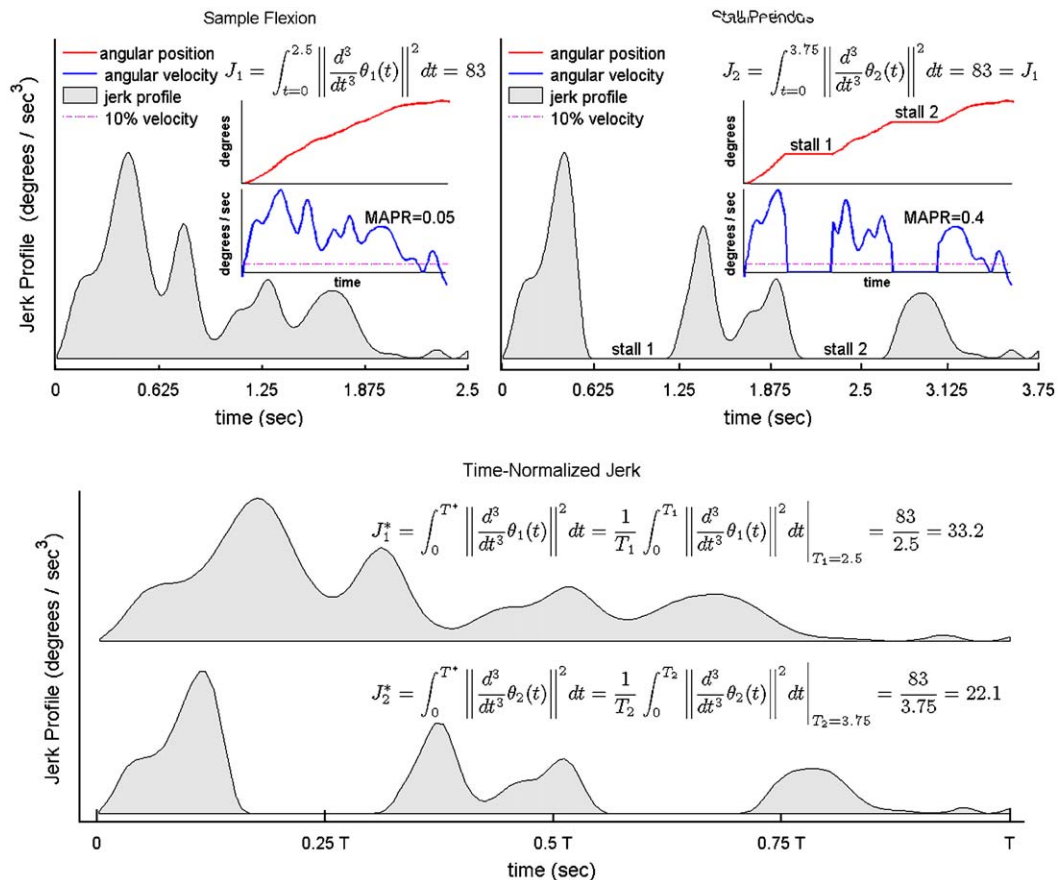


**Fig. 6.** Artefactual deflation of normalized jerk calculation due to stall behavior. Sample flexion motion from healthy subject is evaluated for integrated jerk before and after a simulated stall at two intermediate angles, yielding identical IAJ values (Top). Normalization is necessary to eliminate inter-subject differences in average velocity and range of motion, but cause an artefactual decrease in jerk integral by narrowing peaks to accommodate zero-acceleration periods (Bottom). Trace<sub>1</sub> and Trace<sub>2</sub> are identical, except for intervening spaces. Jerk score is dimensionless, and reflects amplitude-normalized trajectory trace and derivatives.

By measuring unique loci in the angular domain, of which a stall corresponds to a single locus, SAT metrics are not subject to spurious correlations to average velocity:  $|\rho(RED, \dot{\theta})|$ ,  $|\rho(PME_S, \dot{\theta})| < 0.4$  in both cohorts. We conclude that transforming kinematic data into the angular domain yields accurate, high-resolution maps of spontaneous accelerations, and scalar measures of movement smoothness that are insensitive to movement speed, distance, and periods of arrested motion.

### Conflicts of Interest

The authors declare that there are no relationships which might bias the disclosed information.

### Acknowledgements

Steven Escaldi, D.O. and Eileen Crandall, P.T. for patient administration. Kathryn J De Laurentis, Ph.D. for device design and fabrication. David I. Shreiber, Ph.D. for helpful suggestions. Gautam Natarajan, B.S. and Wajdi Kanj, B.S. for technical assistance. Fellowship support for M.W. provided by NSF-IGERT: Integratively Engineered Bionterfaces (DGE 033196, Prabhas Moghe, P.I.), and a RERC grant to W.C. from NIDRR.

### References

- Beppu, H., Suda, M., Tanaka, R., 1984. Analysis of cerebellar motor disorders by visually guided elbow tracking movement. *Brain* 107, 787–809.
- Cozens, J.A., Bhakta, B.B., 2003. Measuring movement irregularity in the upper motor neurone syndrome using normalized average rectified jerk. *Journal of Electromyography and Kinesiology* 13, 73–81.
- Dabroom, A.M., Khalil, H.K., 1999. Discrete-time implementation of high-gain observers for numerical differentiation. *International Journal of Control* 72 (17), 1523–1537.
- Engelbrecht, S.E., 2001. Minimum principles in motor control. *Journal of Mathematical Psychology* 45, 497–542.
- Goldvasser, D., McGibbon, C.A., Krebs, D.E., 2001. High curvature and jerk analyses of arm ataxia. *Biological Cybernetics* 84, 85–90.
- Gottlieb, G.L., Chen, C.-H., Corcos, D.M., 2004. Nonlinear control of movement distance at the human elbow. *Experimental Brain Research* 112 (2), 289–297.
- Hoff, B., 1994. A model of duration in normal and perturbed movement. *Biological Cybernetics* 71, 481–488.
- Hsiang, S.M., Chang, C.C., McGorry, R.W., 1999. Development of a set of equations describing joint trajectories during para-sagittal lifting. *Journal of Biomechanics* 32 (8), 871–876.
- Hu, X., Tong, K., Tsang, V.S., Song, R., 2006. Joint-angle-dependent neuromuscular dysfunctions at the wrist in persons after stroke. *Archives of Physical Medicine and Rehabilitation* 87 (5), 671–679.
- Ju, M.S., Lin, C.C.K., Chen, J.R., Cheng, H.S., Lin, C.W., 2002. Performance of elbow tracking under constant torque disturbance in normotonic stroke patients and normal subjects. *Clinical Biomechanics* 17, 640–649.
- Kahn, L.E., Zygmant, M.L., Rymer, W.Z., Reinkensmeyer, D.J., 2001. Effect of robot-assisted and unassisted exercise on functional reaching in chronic hemiparesis. In: *Proceedings of the 23rd Annual International Conference of the Institute of Electrical and Electronics Engineers/Engineering in Medicine and Biology Society*. Istanbul, Turkey.
- Kashima, T., Isurugi, Y., Shima, M., 2000. Analysis of a muscular control system in human movements. *Biological Cybernetics* 82, 123–131.
- Krebs, H.L., Aisen, M.L., Volpe, B.T., Hogan, N., 1999. Quantization of continuous arm movements in humans with brain injury. In: *Proceedings of the National Academy of Sciences* 96(8), 4645–4649.

- Lan, N., Crago, P.E., 1994. Optimal control of antagonistic muscle stiffness during voluntary movements. *Biological Cybernetics* 71 (2), 123–135.
- Levin, M.F., Dimov, M., 1997. Spatial zones for muscle coactivation and the control of postural stability. *Brain Research* 757, 43–59.
- Levin, M.F., Selles, R.W., Verheul, M.H.G., Meijer, O.G., 2000. Deficits in the coordination of agonist and antagonist muscles in stroke patients: implications for normal motor control. *Brain Research* 853, 325–369.
- Pigeon, P., Yahia, L., Feldman, A.G., 1996. Moment arms and lengths of human upper limb muscles as functions of joint angles. *Journal of Biomechanics* 29 (10), 1365–1370.
- Platz, T., Denzler, P., Kaden, B., Mauritz, K.-H., 1994. Motor learning after recovery from hemiparesis. *Neuropsychologia* 32, 1209–1223.
- Rohrer, B., Fasoli, S., Krebs, H.I., Hughes, R., Volpe, B., Frontera, W.R., Stein, J., Hogan, N., 2002. Movement smoothness changes during recovery. *Journal of Neuroscience* 22 (18), 8297–8304.
- Suzuki, M., Shiller, D.M., Gribble, P.L., Ostry, D.J., 2001. Relationship between cocontraction, movement kinematics and phasic muscle activity in single-joint arm movement. *Experimental Brain Research* 140, 171–181.
- Trombly, C.A., 1993. Observations of improvement in reaching in five subjects with left hemiparesis. *Journal of Neurology, Neurosurgery, & Psychiatry* 56, 40–45.